Shamaei, Farhang; Bergström, Martin; Li, Fang; Taylor, Rocky; Kujala, Pentti

Local pressures for ships in ice

Published in:
Marine Structures

DOI:
10.1016/j.marstruc.2020.102822

Published: 01/11/2020

Document Version
Publisher's PDF, also known as Version of record

Marine Structures 74 (2020) 102822

Contents lists available at ScienceDirect

Marine Structures

journal homepage: http://www.elsevier.com/locate/marstruc

Local pressures for ships in ice: Probabilistic analysis of full-scale line-load data

Farhang Shamaei [a], Martin Bergström [a,*], Fang Li [a], Rocky Taylor [b], Pentti Kujala [a]

[a] Aalto University, School of Engineering, Finland
[b] Memorial University of Newfoundland, Faculty of Engineering and Applied Science, Canada

ARTICLE INFO

Keywords:
Arctic shipping
Arctic ships
Ice loads
Ice pressure
Ship design tools
Event-maximum method

ABSTRACT

Ships operating in ice might be exposed to significant ice loading. Using a probabilistic semi-empirical method known as the event-maximum method, the long-term maximum level of ice loading on a ship can be estimated based on parent distributions of short-term full-scale ice load measurements. The event-maximum method is used to model the relationship between extreme local ice pressures and impact area by estimating parameters corresponding to the inverse slope (α) and intercept (x_0) for the line of best fit for the tail of ranked peak pressure data versus the natural logarithm of the Weibull plotting position. These best-fit lines are assumed to follow an exponential distribution and associated α and x_0 values are produced for different local design areas. This allows for the determination of α-area curves, which reflects the relationship between ice pressure and the local design area. Previous studies have determined α-area curves for different geographical areas such as the Beaufort Sea and South Bering Sea, representing different ice types including both first-year and multi-year ice. In this study, two separate sets of full-scale ice load measurements having been considered, namely measurements from the Kara Sea and the Barents Sea, as well as measurements from the Antarctic Ocean. Using these two datasets, two new α-area curves have been generated that represent among other operating areas (the Kara Sea and the Barents Sea), operating modes (icebreaker assisted operation) and impact areas (aft shoulder) not covered by other curves. Earlier formulations of the event-maximum method are based on local design areas in which the width and height of areas are defined by the size of instrumented rectangular panel areas (or combinations of those areas) on the bow of the vessel from which the data were collected. In that approach, ice thickness is not directly considered since the height of individual panels is based on the dimensions of instrumented areas and moreover, detailed ice thickness records were not available for those data sets. In the present study, an alternative approach has been developed to extend the event maximum method for use with ship line-load data. In this approach ice pressures are calculated by dividing the ice force measured on frames by the corresponding line-load area (A_{LL}), which is the product of the width (W) that is based on frame spacing and an assumed line-load height (H) corresponding to 30% of the maximum prevailing ice thickness, as per best design practice, along the lines of the Finnish-Swedish ice class rules. Data already presented as line-loads (in units of force per unit width), are converted to pressures by dividing line-loads by height H. The event definition used in the present approach is defined as the maximum pressure corresponding to 10- or 20-min intervals, as

Abbreviations: HPZ, High Pressure Zone.

* Corresponding author. Aalto University, School of Engineering, Marine Technology, P.O. Box 15300, 00076, Aalto, Finland.
E-mail addresses: farhang.shamaei@aalto.fi (F. Shamaei), martin.bergstrom@aalto.fi (M. Bergström), fang.li@aalto.fi (F. Li), rstaylor@mun.ca (R. Taylor), pentti.kujala@aalto.fi (P. Kujala).

https://doi.org/10.1016/j.marstruc.2020.102822
Received 20 November 2019; Received in revised form 19 May 2020; Accepted 20 May 2020
Available online 7 August 2020

opposed to the impact event definition used in earlier works. In applying this extended method to develop new α-area curves, valuable insights into the relationship between local peak ice pressure and prevailing ice thickness have been gained for the above-mentioned full-scale measurements. The determined curves indicate a negative correlation between prevailing ice thickness and maximum local nominal ice pressure. Finally, it has been demonstrated that it is feasible to apply such curves in combination with the principle of the event-maximum method to estimate the maximum nominal ice pressure expected for a ship given a specified transit distance in sea ice with different prevailing thicknesses.

Notations

A_{LL}	Line-load area
α	Inverse slope of the best-fitted line to the peak pressures [MPa]
C	Ice condition-specific coefficients
D	Ice condition-specific coefficients
D_t	Distance that ship operates in a specific ice thickness category [NM]
$F_X(x)$	Cumulative Distribution Function of the ice pressures
$F_Z(z)$	Cumulative Distribution Function of the maximum local ice pressure
F	Ice load [kN]
f	Frequency of the ice impacts
H	Load height [m]
h	Ice thickness [m]
L	Load length [m]
μ	Number of ship-ice impacts on a particular line-load area
P	Ice pressure [MPa]
P_e	Probability of exceedance
r	Percentage of the ship-ice impacts hitting the specific hull panel
v	Number of ship-ice impacts during a specific period
X_i	Measured ice pressure value [MPa]
x	Random local ice pressure [MPa]
x_0	Intercept of the best-fitted line with the x-axis [MPa]
Z	Maximum ice pressure [MPa]
z_e	Maximum local ice pressure corresponding to a specific probability of exceedance [MPa]

1. Introduction

1.1. Background

Maritime operations in Arctic waters is on the increase, driven by the extraction of Arctic natural resources, trans-Arctic shipping,

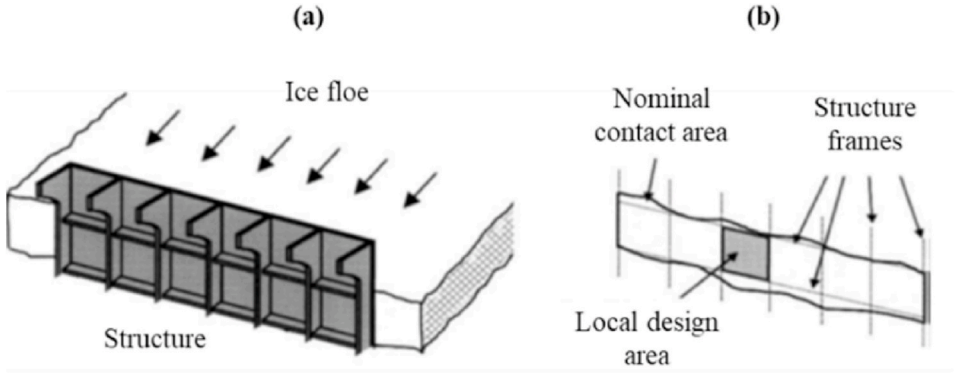

Fig. 1. Illustrations of (a) ice interacting with a vertical-walled structure, and (b) the global interaction and local design areas. Based on Taylor et al. [5].

and Arctic tourism. To ensure a high level of safety, environmental protection, and efficiency, the design and operation of Arctic ships requires the consideration of a whole range of Arctic specific risk factors including sea ice, icing, low temperatures, darkness, high latitude, remoteness, the lack of relevant crew experience, and difficult weather conditions [2]. Among these factors, from a design perspective, sea ice is perhaps the most important as it might expose a ship to very significant ice loading, potentially compromising its structural integrity.

Ice loading is a result of a complex and stochastic ship-ice interaction process with many unknowns [3,4]. Nevertheless, following Taylor et al. [5] as per the schematic illustrations in Fig. 1, two different areas of interest can be defined: (a) nominal (or global) contact area, and (b) local design area. The nominal contact area corresponds to the area of the hull projected onto the original dimensions of the ice feature [6]. The local design area, on the other hand, is typically the area of a plate between frames, i.e., a panel, which is relevant for design purposes [5].

Analyses of full-scale ice load measurements by Sanderson [7]; Frederking et al. [8]; and Daley et al. [9]; indicate that in ship-ice interactions, because in such interactions ice fails primarily by crushing, the distribution of ice pressure on the ship-ice interaction area is highly in homogeneous. As a result, within any global interaction area, there will be highly concentrated forces on localized contact areas, known as High Pressure Zones (HPZs) [10]. The total force acting over any global interaction area or within a local design area is the sum of simultaneous HPZ forces as well as any force transmitted through regions of crushed ice in the contact zone, which may be modeled as a lower background pressure, see e.g. Ref. [11]. Since detailed information about HPZs (e.g. number, size, location, intensity) is typically not available for most ice interaction datasets, local ice pressures are typically calculated as the spatial average of the total force on a given panel, averaged over that corresponding area [12]. As demonstrated by Ref. [5], among others, random HPZ forces result in a scale-effect such that average pressures on a larger areas average out to be smaller than those on smaller areas. This reflects that in a ship-ice interaction, the maximum HPZ may occur on any point within the nominal interaction area [12].

HPZs are highly variable in time and space and the resulting peak pressures vary significantly [12]. In accordance with multiple studies including Kujala & Vuorio [13]; Jordaan et al. [6]; Suominen and Kujala [14]; Suyuthi et al. [15]; and Kotilainen et al. [16]; nominal ice pressure peaks tend to follow a Weibull or exponential distribution. Accordingly, a ship operating in ice is at risk of being exposed to rare but extreme ice loads that are significantly higher than normal loads.

To account for the above-mentioned scale-effect and stochastic nature of ice loading, Jordaan et al. [6] present a semi-empirical probabilistic method, known as the event-maximum method. As demonstrated by Taylor et al. [5]; the event-maximum method can be used to estimate the relationship between the maximum ice pressure acting on local areas of a ship hull, and the ship's ice exposure, quantified in terms of the numbers of impacts with different types of ice hitting the area in question. The relationship between the local ice pressure and the local design area is described in terms of so-called α-area curves, which are empirically determined based on parent distributions of full-scale ice load measurements. Thus, the application of the method is limited by the availability of relevant α-area curves.

Taylor et al. [5] present α-area curves for in total 11 different voyages representing different ice conditions. Ice conditions related to the different measurements are described in terms of sea area and date (e.g. the Beaufort Sea – November–December 1984, South Bering Sea – March 1983) and the prevailing type of ice (e.g. multi-year ice, first-year ice).

The event maximum method as proposed and supported by Taylor et al. [5] was focused primarily on the analysis of ice load data to develop design relationships for offshore engineering applications. Consequently, when considering the application of this approach to other ship-ice data sets, additional considerations are needed. First, the α-area curves produced by Taylor et al. [5] were determined using data obtained from measurements on the bow area, which typically is the most exposed in terms of ice loading. Nevertheless, when designing an Arctic ship, designers must consider ice loading on other parts of the hull as well. While areal exposure factors may be used to adjust design ice pressures to account for differences in exposure to ice for locations other than the bow, it is worthwhile to analyze data from measurements at other hull locations, when such data are available. Second, the available α-area curves were determined based on measurements from independently operating ships. In other words, they do not account for the effect of icebreaker assistance. Third, since this method is based on local design areas, where the area is defined in terms of the width and height of the instrumented panels, the approach does not directly consider the effect of prevailing ice thickness. Naturally, this makes it is difficult to directly assess the effect of annual and local variations in ice thickness, among other factors. Finally, the event definition used in Taylor et al. [5] was based on individual impact events that the analysts identified and extracted from the panel pressure-time series data. This definition differs from the 10- and 20-min maximum line-load events from ship-ice data considered here, as is explored further later in this paper.

In light of this background, some modifications of this methodology have been proposed here to allow for analysis of two separate sets of full-scale ice load measurements from the Kara and Barents Seas, as well as data from the Antarctic Ocean. These data have been analyzed here with the aim of developing two new α-area curves that represent operating areas (the Kara Sea and the Barents Sea), operating modes (icebreaker assistance) and hull regions (aft shoulder) not included in earlier analyses. In addition to extending the methodology to allow for analysis of these additional datasets, it is also possible to confirm that ice load measurement conducted in similar conditions but by different techniques produce similar results. Using the extended event-maximum method, the effect of sea ice thickness may be considered by examining the direct relationship between local ice pressure and prevailing ice thicknesses. Furthermore, it is possible to assess the utility of such a relationship for providing a probabilistic estimate of the maximum line-load pressure on a ship transiting a certain distance in ice of various prevailing thicknesses and types.

Specifically, the study aims to address the following Research Questions (RQ):

- RQ 1: How do α-area curves and related peak ice pressure estimates depend on factors such as impact location and the use of icebreaker assistance?

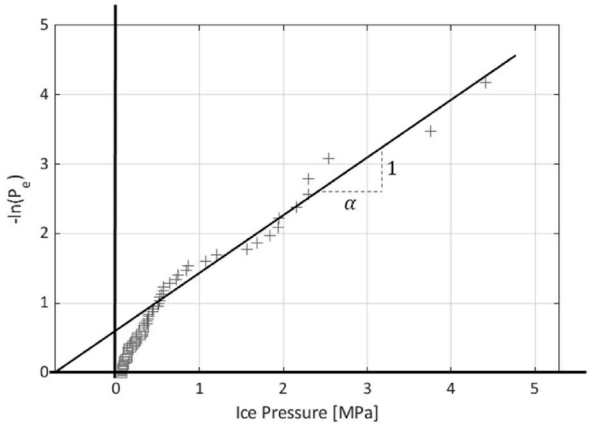

Fig. 2. Example of lines fitted to the ranked peak pressures on the bow (#134 + 400) of MV S.A. Agulhas II for a specific range of prevailing ice thickness (0.7 m < h≤1.2 m). The data originate from interactions with all types of sea ice features including ridges. The prevailing ice thickness should be considered descriptive of the overall ice conditions in the area.

- RQ 2: What is the relationship between α-area ice pressure curves and prevailing ice thickness?
- RQ 3: Is it feasible to estimate the maximum nominal ice pressure on a ship based on its distance covered in sea ice of various thickness?

The study is limited to analyzing the relationship between peak (nominal) ice pressure and the prevailing ice thickness. The considered ice pressure data is based on full-scale ice loads measurements covering all types of ship-ice interactions including impacts with ice ridges. Therefore, the study does not aim to consider the effect of any individual sea ice features (e.g. level ice, ice ridges). Also, the study does not aim to consider compressive ice loads that a ship might be exposed to if it becomes beset in ice. The considered data on the prevailing ice thickness is based on visual observations and used as an index representing the overall ice conditions in an area.

By assuming, along the lines of Traficom [17]; that the ice load height is 30% of the prevailing maximum ice thickness, a direct relationship between the estimated nominal ice pressure and the ice line-load of a ship can be established. This makes the study relevant in the context of goal-based structural design of Arctic ships, as supported by the International Code for Ships Operating in Polar Waters (Polar Code) [2]. While this study is not directly focused on current ship design rules other than the Polar Code, it should be noted that the event-maximum method is included in the recommended methods in the ISO 19906:2010 standard for offshore structures [18].

1.2. Description of the event-maximum method

The event-maximum method by Jordaan et al. [6] makes it possible to probabilistically assess the maximum local ice pressure acting on a particular local design area. The method implies that the local ice pressure can be obtained by fitting a line to a set of ranked measured peak pressures for a particular area plotted against the natural logarithm of the Weibull plotting position [6]. The best-fitted line is assumed to follow an exponential distribution as per Eq. 1

$$F_X(x) = 1 - \exp\left(-\frac{x - x_0}{\alpha}\right), \tag{1}$$

where x is a random local ice pressure [6]. Parameters x_0 and α are constants for a specific area describing the intercept of the best-fitted line with the x-axis and the inverse slope of that line respectively as shown in Fig. 2 [5].

The maximum pressure Z on a particular area is defined in accordance with

$$\boldsymbol{Z} = \max(\boldsymbol{X}_1, \boldsymbol{X}_2, \ldots, \boldsymbol{X}_N), \tag{2}$$

where X_i is a measured pressure value and N is the total number of impacts [6]. By using extreme statistics to Eq. (1), the cumulative distribution function of the maximum local ice pressure for a panel area may be obtained in accordance with

$$\boldsymbol{F}_Z(z) = \mathbf{exp}\left\{-\mathbf{exp}\left(-\frac{(z - \boldsymbol{x}_0 - \boldsymbol{x}_1)}{\boldsymbol{\alpha}}\right)\right\}, \tag{3}$$

where $x_1 = \alpha(ln\mu)$ and μ denotes the ice exposure. Ice exposure is determined in terms of the number of ship-ice impacts on a particular panel area as per

$$\boldsymbol{\mu} = \boldsymbol{v}^{*}\boldsymbol{r}, \tag{4}$$

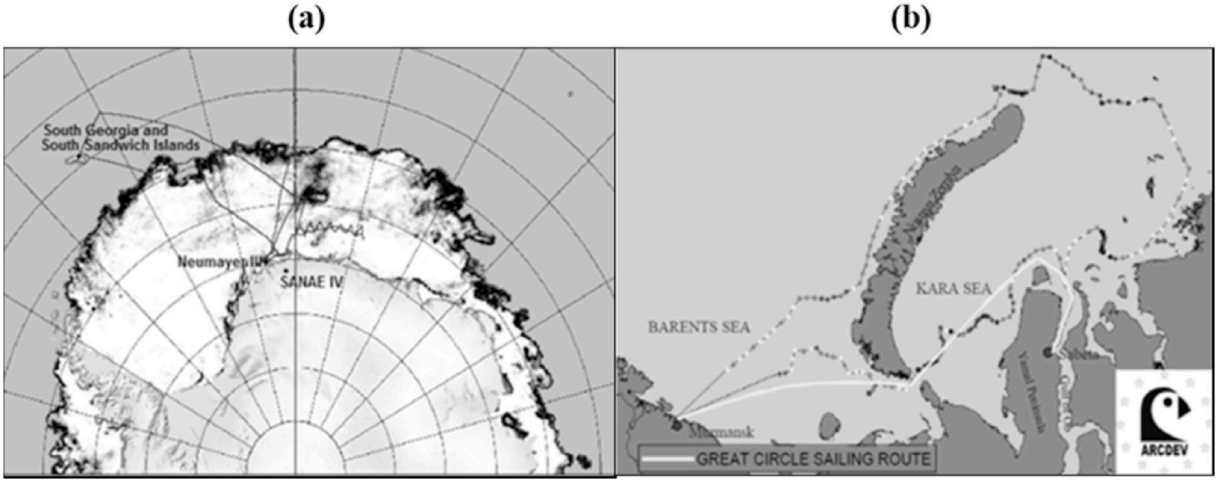

Fig. 3. (a) Voyage of MV S.A. Agulhas II [11], (b) Voyage of MV Uikku [1].

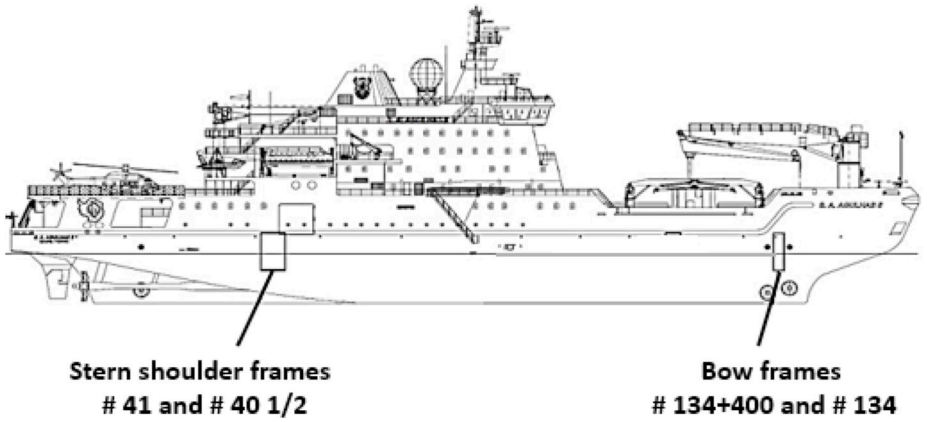

Fig. 4. Strain gauges on MV S.A. Agulhas II [20].

where (v) is the number of ship-ice impacts during a specific period (e.g. one year), and (r) is the percentage of the ship-ice impacts hitting the specific hull panel in consideration [5]. The number of impacts can either be estimated empirically based on full-scale ice load measurements or semi-empirically, for instance by applying the simulation-based approach proposed by Bergström et al. [19].

The parameter α is assumed to be dependent on the panel area, which represents the decrease of ice pressure with respect to the area following

$$\alpha = CA^D, \tag{5}$$

where A denotes the local design area and $C$and D are ice condition specific coefficients [6]. Therefore, the method is dependent on the coefficients C and D, which need to be empirically determined for different ice conditions and geographical regions. Taylor et al. [5] applied the event-maximum method to sets of full-scale ice pressure and load measurements and determined thereby a set of α-area curves for various ice conditions (e.g. first-year ice, multi-year ice) and sea areas (e.g. Beaufort Sea, Bering Sea, and Antarctic Sea). However, there are still significant sea areas such as the Baltic Sea, the Barents Sea, and the Kara Sea for which no α-area curves are available.

Based on the above, in accordance with Taylor et al. [5]; the maximum local ice pressure (z_e) on a ship's hull, for a specific probability of exceedance and area, can be calculated per

$$z_e = x_0 + \alpha \{ -\ln[-\ln F_Z(z_e)] + \ln \mu \} \tag{6}$$

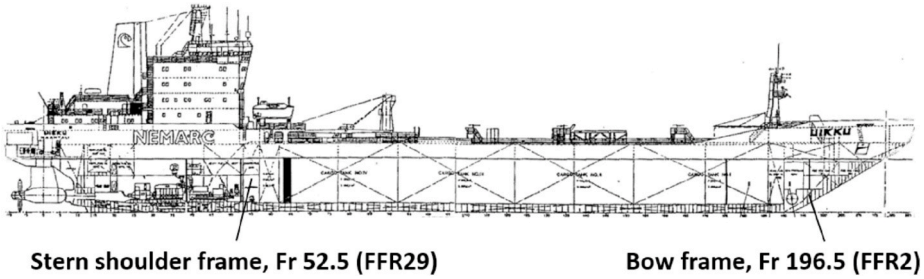

Fig. 5. Strain gauges on MV Uikku [22].

Table 1
The ice thickness categories for the measurements on MV S.A. Agulhas II.

Ice thickness category	Category A1	Category A2	Category A3
Ice thickness (m)	$0.7< h \leq 1.2$	$1.2< h \leq 2$	$h > 2$
Mean value (m)	0.95	1.6	2.75

Table 2
The ice thickness categories for the measurements on MV Uikku.

Ice thickness category	Category B1	Category B2	Category B3
Ice thickness (m)	$0.1< h \leq 0.3$	$0.3< h \leq 0.7$	h>0.7
Mean value (m)	0.2	0.5	1.1

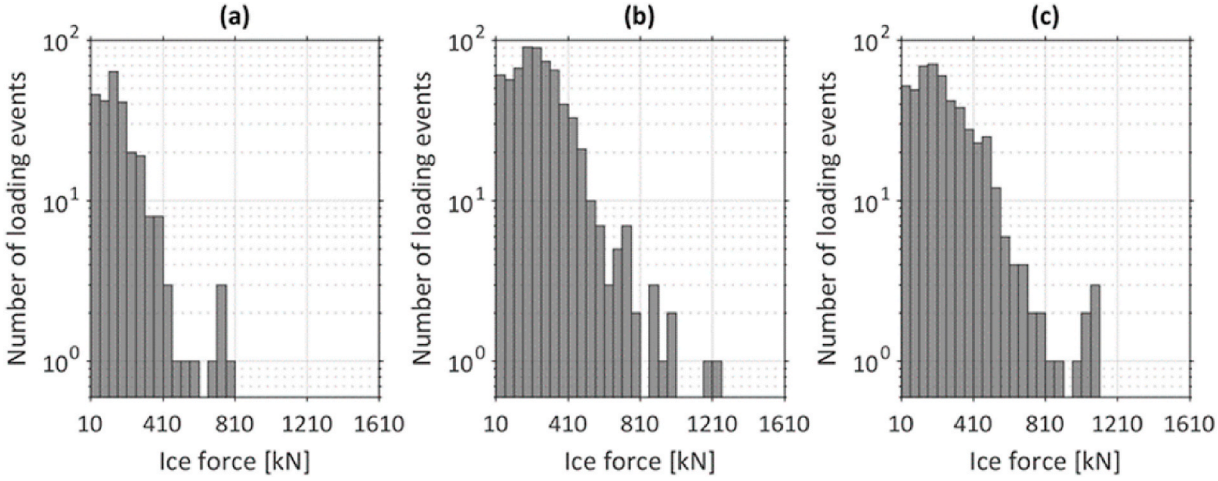

Fig. 6. Example of 10-min maximum ice loads on the bow area of MV S.A. Agulhas II (#134 + 400) for different ice thicknesses: (a) 0.7 m < $h \leq$1.2 m, (b) 1.2 m < $h \leq$2 m, (c) h > 2 m. Each column represents an ice force range of 50 kN.

2. Analysis

2.1. Overview of full-scale ship-ice load datasets

Towards addressing the research questions, two different series of full-scale ice load measurements have been considered: (a) measurements recorded on MV S.A. Agulhas II on a voyage across the Antarctic Ocean in 11/2013–02/2014, and (b) measurements recorded on MV Uikku on a voyage across the Barents Sea and the Kara Sea in 04–05/1998. Both ships encountered mainly first-year ice, but it is possible that some of the first-year ice encountered by MV S.A. Agulhas II included old ice inclusions. During the measurements, MV S.A. Agulhas II operated independently in ice, i.e. it received no icebreaker assistance, whereas MV Uikku was assisted by an icebreaker. Both voyages are plotted in Fig. 3.

During the voyages, the ships were instrumented with strain gauges at the bow and the stern shoulder in accordance with Fig. 4 and

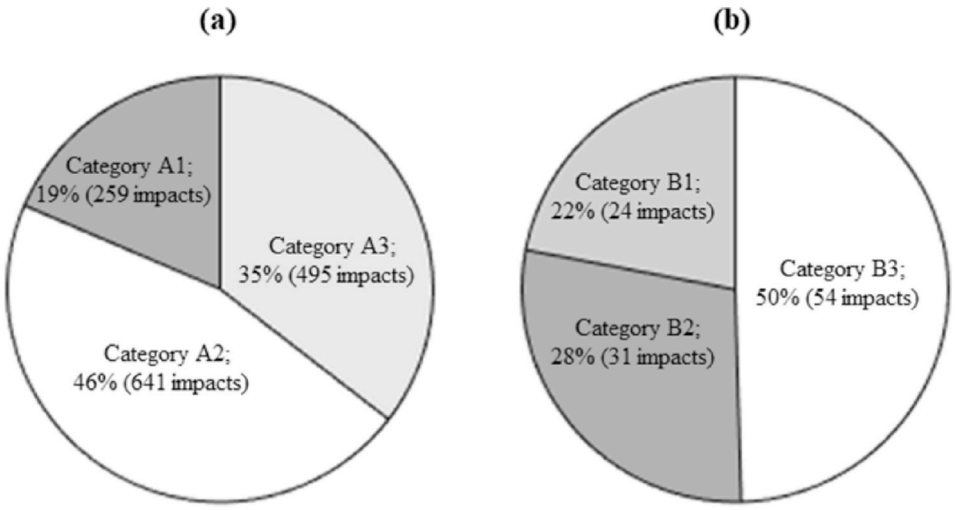

Fig. 7. Distribution of (a) 10-min maximum ice thickness observations related to the ice load measurements on MV S.A. Agulhas II (bow area, frame #134), (b) 20-min maximum ice thickness observations related to the ice load measurements on MV Uikku (bow area, FFR2).

Fig. 5. Ice thickness data was recorded based on visual observations [20].

2.2. Distribution of ice loads and thicknesses

Ice load events (load amplitudes) from the full-scale ice load measurements were extracted using the method developed by Hänninen et al. [21]. Accordingly, based on the available full-scale data, 10-min maximum ice loads at the bow and the stern shoulder of MV S.A. Agulhas II were calculated for different ice thicknesses categories defined per Table 1. Using the same method, 20-min maximum ice loads at the bow and the stern shoulder of MV Uikku were calculated for different ice thicknesses categories defined per Table 2 [22]. The difference in the load amplitude interval (10-min vs. 20-minutes) relates to differences in the full-scale measurements. To exclude noise such as wave loads, a lower threshold of 10 kN was applied on both data sets.

It should be noted that the ice thickness categories defined per Tables 1–2 are specific to each set of full-scale ice load measurements. As explained in the following, this is needed to enable the determination of three α-area points for each set of data. Examples of ice load data determined in accordance with the above are presented in Fig. 6.

An assumption made in this analysis is that the peak loads during a given period correspond to the impact with the thickest ice feature that impacted the vessel during the period. As a result, each considered load amplitude was paired to the maximum ice thickness observed during the same period. Fig. 7 presents the distribution of the 10- and 20-min maximum ice thickness observations related to the ice load measurements on the bow areas of MV S.A. Agulhas II and MV Uikku. As per the figure, the ice load measurements from MV S.A. Agulhas II and MV Uikku includes 1395 and 109 considered ice load events, respectively.

The loads are measured based on all types of ship-ice interactions, including impacts with ridges. Differentiation between different ice features is neither needed nor possible since the hull response captures 100% of the load from all types of interactions. This means that the considered ice thickness in effect acts as an index for the overall ice conditions in the area.

2.3. Determination of ice pressure

Since the two noted full-scale datasets do not include direct ice pressure measurements, the ice pressures are instead calculated based on measured forces acting between instrumented frames. As noted above, it has been assumed that each measured 10- or 20-min maximum ice load corresponds to the maximum ice thickness category observed during the same period. As per best design practice, along the lines of the Finnish-Swedish ice class rules, it is also assumed that the height of the actual ship-ice interaction area, i.e. the line-load height (H), is 30% of the maximum prevailing ice thickness [17]. It is important to note that the definition of the area used here to estimate the local ice pressure is not the same as the local design area used in Jordaan et al. [6] or Taylor et al. [5]; which is based on panel dimensions. Rather a new area definition is defined here as the local line-load area A_{LL} which is the product of the load length (L) and line-load height H, as described above. For MV S.A. Agulhas II, for which measured ice loads are determined in terms of the total 10-min maximum ice load (F) [kN], it has been assumed that the load length (L) is equal to the ship frame spacing of 0.4 m. For MV Uikku, no assumptions regarding load length are required since the measured ice loads have already been normalized per unit length and recorded in terms of 20-min maximum line loads (F/L) [kN/m]. Based on this information, the ice pressures (P) have been calculated using as:

$$P = \frac{F}{A_{LL}} = \frac{F}{L^{*}H} = \frac{F}{L}{}^{*}\frac{1}{H}\left[\frac{kN}{m^2}\right] \tag{7}$$

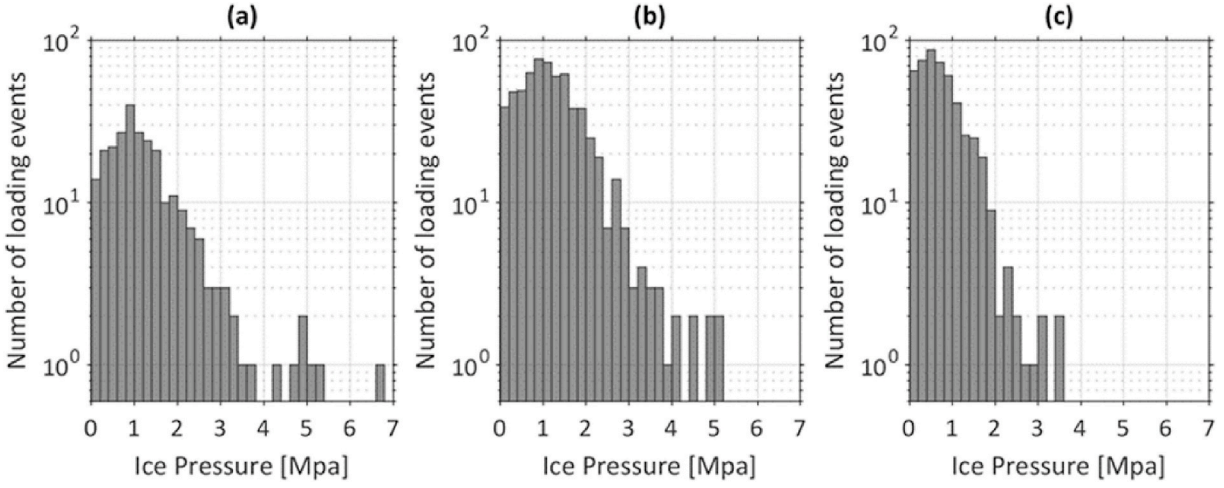

Fig. 8. Example of calculated 10-min maximum ice pressures on the bow (#134 + 400) of MV S.A. Agulhas II for different ice thicknesses; (a) 0.7 m $< h \leq$1.2 m, (b) 1.2 m $< h \leq$2 m, (c) $h >$ 2 m. Each column represents an ice pressure range of 50 kN.

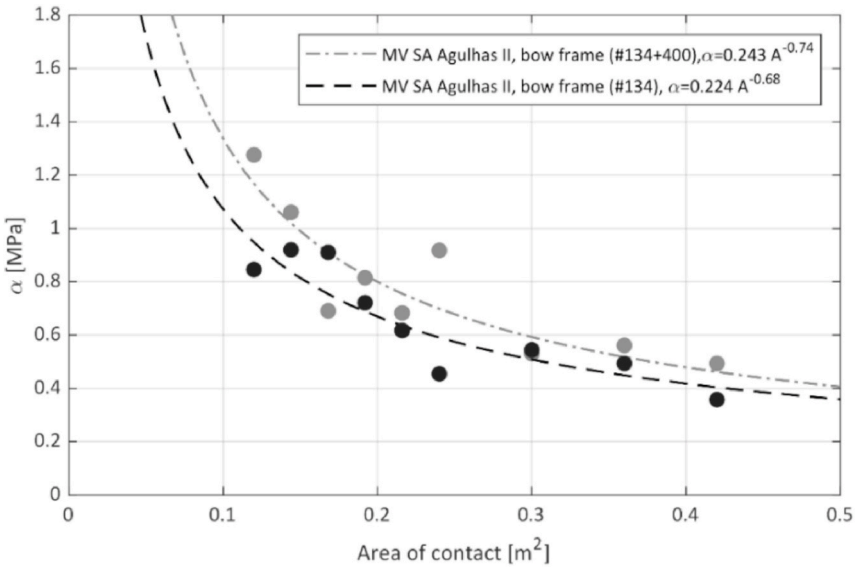

Fig. 9. Example of obtained α-area relationships and related α-area curves. The area of contact equals here the line-load area A_{LL}.

In accordance with the above, 10- and 20-min maximum ice pressures have been calculated for the different ice thicknesses categories and hull locations (frames). Examples of ice pressure values calculated in this manner are shown in Fig. 8.

The normalization of equivalent pressures by the nominal level ice thickness is a necessary simplifying assumption since it is not possible to know the exact ice thicknesses for every interaction. It is worth noting that for ridges this is a conservative assumption since this assumes that all the measured ridge load is distributed over the estimated level ice thickness when in fact it may be distributed over a larger thickness.

2.4. Relationship between local ice pressure and line-load area

In response to RQ 1, to determine α-area curves for different hull regions and operating modes, the event-maximum method has been applied to the noted two sets of full-scale ice load measurements. Values of Z, $F_Z(z)$, x_0, and α were then determined as described above. In addition, the relationship between nominal ice pressure and contact area was determined in accordance with Eq. (5). Accordingly, following the example presented in Fig. 2, α-values were first defined for a set of specific areas from linear curve fits to the tail of the cumulative distribution function of the calculated ice pressures. For the purpose of curve-fitting in the present analysis, the tail of the data is taken as those data in the ranked ice pressures that are greater than the median. The obtained α-values were then plotted against their corresponding area values. Power law curves were next fitted to these α-area data using least-squares regression

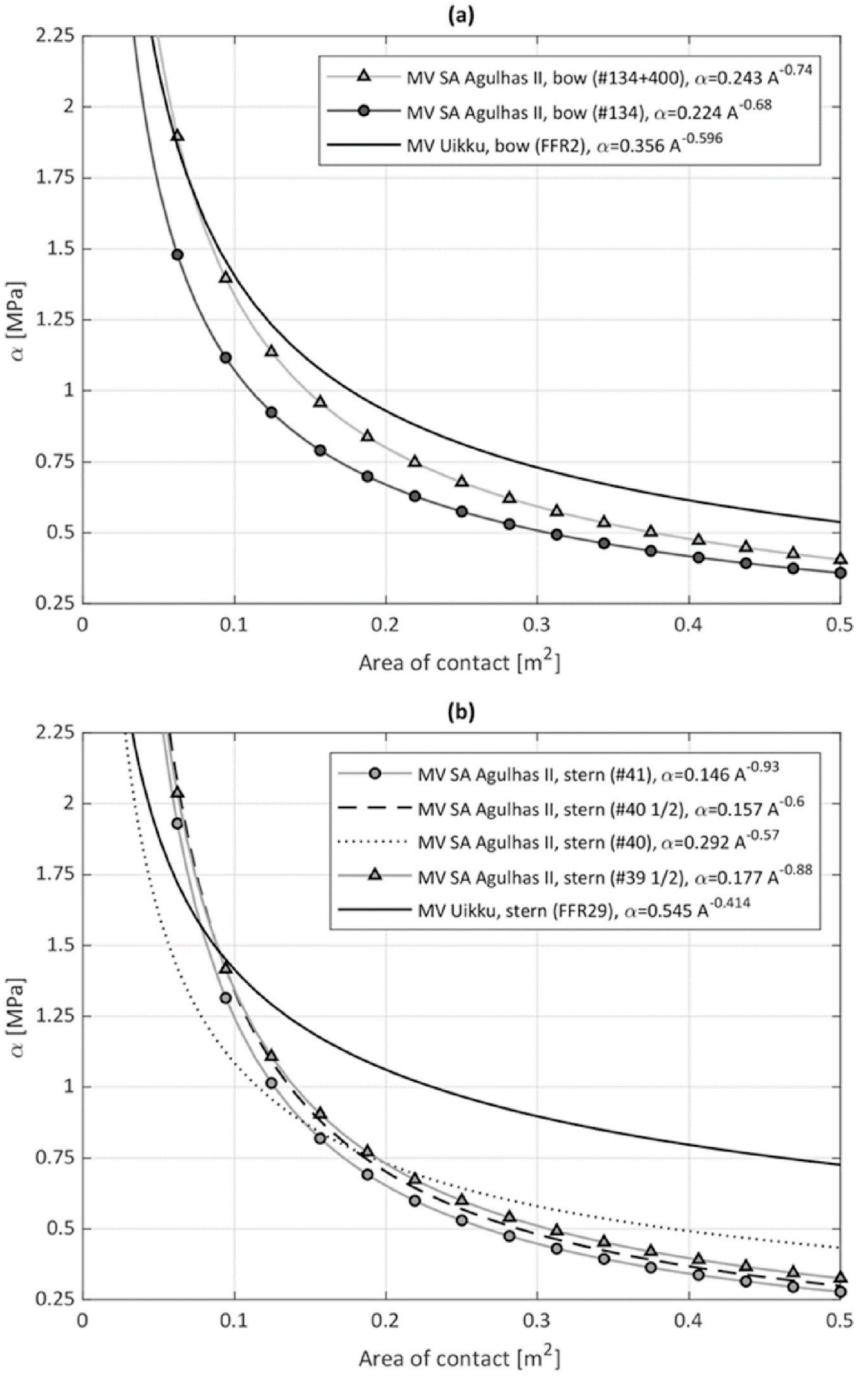

Fig. 10. Obtained α-area curves for (a) the bow area and (b) the stern shoulder area of MV S.A. Agulhas II and MV Uikku. Area of contact equals here the line-load area A_{LL}.

fitting, to estimate the corresponding coefficient C and exponent D values from Eq. (5) needed to define the α-area relationship for each analysis case. These data were then plotted along with the corresponding α-area curve, as shown in Fig. 9 for the example plot for measurements recorded at the bow area of MV S.A. Agulhas II (Shamaei et al., [23].

To investigate the influence of measurement location and operating mode on the expected ice pressures, α-area curves calculated for different hull locations (frames), namely the bow and the stern shoulder were plotted in Fig. 10. The curves determined based on measurements conducted on MV S.A. Agulhas II represent independent operation, whereas those determined based on measurements conducted on MV Uikku represent icebreaker assisted operation.

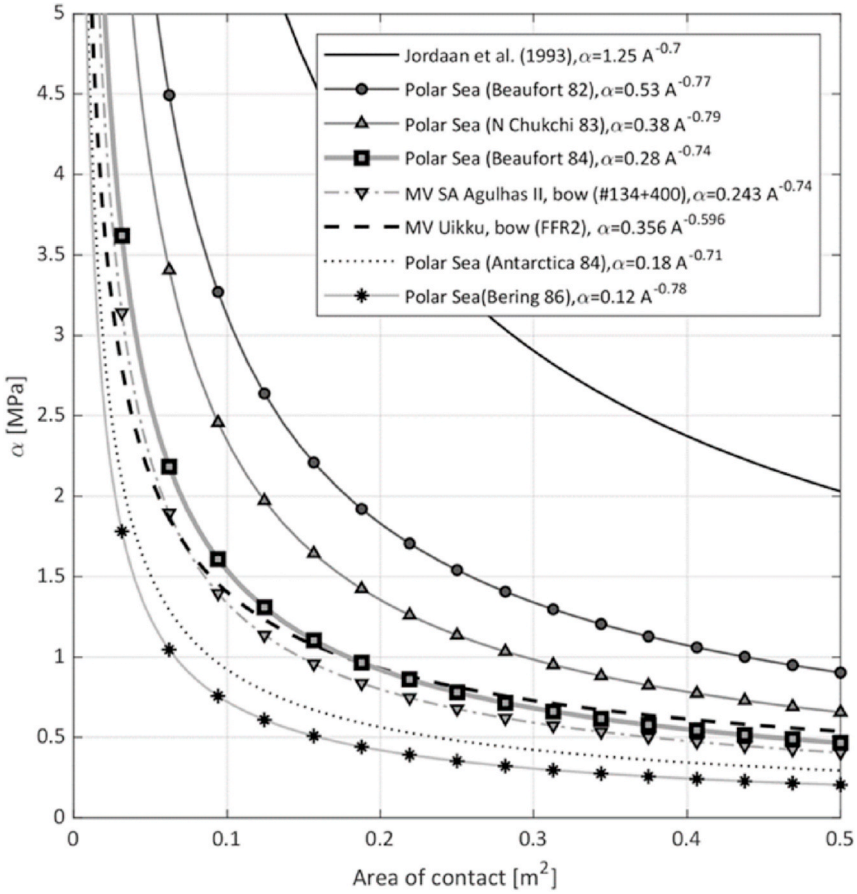

Fig. 11. Comparison of α-area curves determined for the bow area of MV S.A. Agulhas II and MV Uikku with corresponding α-area curves determined by Ref. [5] for different ships and operating areas. The legend presents the curves in descending order as shown in the plot. Area of contact equals the line-load area A_{LL}.

From Fig. 10 it may be seen that all but one of the α-area curves representing the stern shoulder are close to those representing the bow area. Accordingly, if subjected to the same number of ice impacts, both areas are expected to be subject to the same level of ice loading. Notwithstanding, by comparing individual α-area curves representing nearby frames on the same ship (e.g. frame #41 and #40 ½ of MV SA Agulhas II), significant variations are found. This can be explained by the stochastic nature of the ice loading process, as well as by possible instrumentation related issues. The need to consider such local variations in ice loading is reflected for instance in the International Association of Classification Societies (IACS) Polar Class (PC) rules, which require ice loads at the bow area to be determined based on the maximum of ice load parameters calculated for at least four sub-regions at the bow [24].

From Fig. 10 it can also be seen that the curves representing MV Uikku are generally close to those representing MV SA Agulhas II. However, for contact areas above around 0.1 m^2, the curves representing MV Uikku are slightly above those representing MV SA Agulhas II, which is surprising given that MV Uikku, in contrary to MV SA Agulhas II, was assisted by an icebreaker. This finding can in part be explained by differences in hull form, and in part by the fact that the ice load data measured on MV Uikku represents 20-min maximum ice loads, whereas the ice load data measured on MV SA Agulhas II represents 10-min maximum ice loads. In addition, most of the measurements from MV Uikku represent line-load areas below 0.1 m^2, resulting in increased uncertainty in α-values for larger line-load areas determined by curve fitting.

In Fig. 11, α-area curves calculated for the bow area of MV S.A. Agulhas II and MV Uikku, are compared with α-area curves presented by Taylor et al. [5]. The curves presented by Taylor et al. [5] were all determined based on ice load measured at the bow area of different ships operating in different ice conditions. From Fig. 11 it may be seen that the α-area curves determined for the bow area of MV S.A. Agulhas II and MV Uikku are, with the exception of the design curve for offshore structures proposed by Jordaan et al. (1993), in the same range and have the same shape as those presented by Taylor et al. [5]. This indicates that the event-maximum maximum method is stable and consistent.

Fig. 12 demonstrates how the determined α-area curves can be applied in accordance with Eq. (6) to estimate the maximum pressure for various contact areas and return periods. The presented curves are calculated by assuming, as per Table 3, that the total annual number of impacts on the bow of MV SA Agulhas II (#134 + 400) and MV Uikku (FFR2) are 1428 and 109, respectively. The corresponding total annual number of impacts on the stern shoulder of MV SA Agulhas II (#41) and MV Uikku (FFR29) are 1063 and

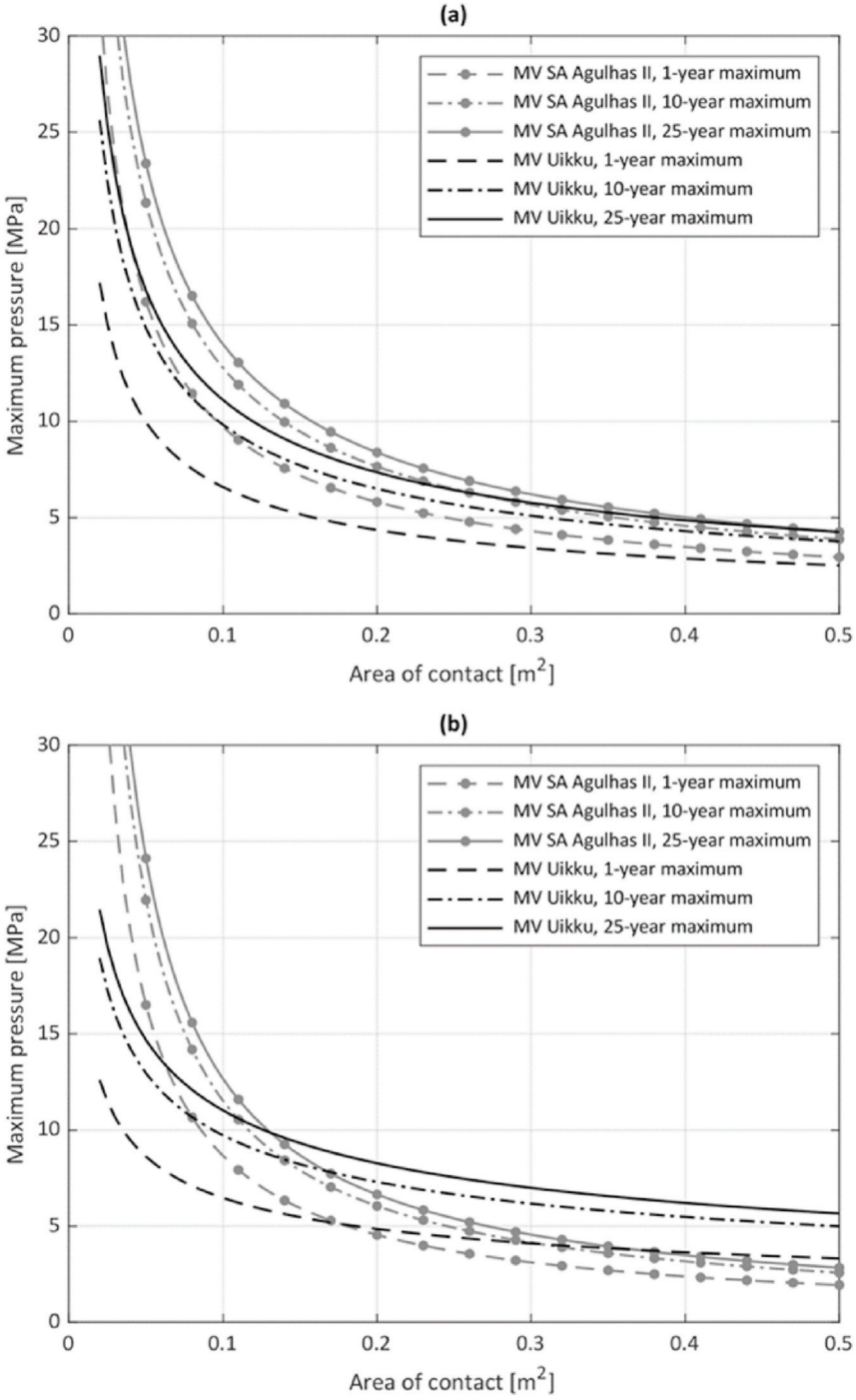

Fig. 12. Calculated maximum local pressures for different return periods and hull areas: (a) the bow area of MV SA Agulhas II (#134 + 400) and MV Uikku (FFR2), (b) the stern shoulder area of MV SA Agulhas II (#41) and MV Uikku (FFR29). Area of contact equals here the line-load area A_{LL}.

97, respectively. As per the figure, for instance the estimated 1- and 25-year maximum ice pressure on an area of 0.1 m^2 on the bow of MV SA Agulhas II (#134 + 400) are approximately 10 MPa and 14 MPa, respectively. The latter is thereby around 40% higher than the former.

2.5. Analysis of the relationship between local ice pressure and ice thickness

In response to RQ 2, the extended event-maximum method has been applied to investigate if this approach can be used to establish a

Table 3
The number of ice impacts per ship, hull area, and ice thickness category.

Ice thickness category	1	2	3
MV S.A. Agulhas II:			
Operational distance in ice [NM]	367	584	245
Average speed in ice [Kn]	7.7	5	3.3
Number of impacts at the bow area	285	699	444
Frequency of impacts at the bow area [1/NM]	0.77	1.19	1.81
Number of impacts at the stern shoulder area	175	529	359
Frequency of impacts at the stern shoulder area [1/NM]	0.47	0.90	1.46
The ratio of bow to stern shoulder impacts	1.64	1.32	1.24
MV Uikku:			
Operational distance in ice [NM]	93	98	148
Average speed in ice [Kn]	11.6	9.4	8.2
Number of impacts at the bow area	24	31	54
Frequency of impacts at the bow area [1/NM]	0.25	0.31	0.36
Number of impacts at the stern shoulder area	16	28	53
Frequency of impacts at the stern shoulder area [1/NM]	0.17	0.28	0.35
The ratio of bow to stern shoulder impacts	1.47	1.11	1.03

direct relationship between nominal ice pressure and ice thickness. To this end, it has been assumed that the local ice pressure associated with a specific ice thickness can be modeled based on the tail of the cumulative distribution function of the full-scale ice pressures vs. ice thickness data. Based on this assumption, the parameters Z, $F_Z(z)$, x_0, and α have been estimated in accordance with the extended event-maximum method, but by using ice thickness as a variable instead of the local line-load area. Correspondingly, the relationship between local ice pressures and ice thickness has been modeled in accordance with

$$\alpha = Ch^D, \tag{8}$$

where h [m] is the ice thickness and $C$and D are ice condition specific dimensionless coefficients. Eq. (8) differs thereby from Eq. (5) in that α is determined with respect to ice thickness (h) instead of with respect to the local line-load area (A).

In order to determine the α–h relationship in accordance with Eq. (8), α-values for a set of specific ice thickness ranges are first calculated following the example presented in Fig. 2, using a linear fit to the tail of the cumulative distribution function of the calculated ice pressures. In this study, the tail of the distribution refers to the ranked ice pressure measurements greater than the median. In this analysis, the obtained α-values are assumed to correspond to the mean thickness of the associated ice thickness categories given in Tables 1 and 2. The specific coefficients C and D for different ice types are found by the least squares regression curve by fitting Eq. (8) to the α-h data for each ice type.

Following the above, a set of α–h curves were also calculated for the bow and the stern shoulder area based on the corresponding full-scale ice load measurements from MV S.A. Agulhas II and MV Uikku. The obtained curves, presented in Fig. 13, indicate that α decreases with increasing ice thickness, i.e. that α and h are negatively dependent. The circles presented in the figure indicate the measured points to which the curves are fitted.

Similarly, based on lines fitted to the ranked peak pressures, x_0 values for various hull areas with respect to the mean ice thickness for each thickness category were calculated, as shown in Fig. 14. As may be observed in this figure, the obtained x_0-values tend towards zero as ice thickness (h) increases. Naturally, this simplifies the application of the method. It is noted that while the x_0 values shown in Fig. 14 may be used to model ice pressures if the design case has the same exposure as the data from which these parameters were derived, and otherwise the x_0 should be adjusted to match the design exposure level (e.g. see [5]).

2.6. Determination of the number of ship-ice impacts

The number of ship-ice impacts μ from the full-scale measurements may be determined separately for different ice thickness categories per

$$\mu = f^* D_t, \tag{9}$$

where f [1/NM] is the frequency of the relevant ice impacts and D [NM] is the distance that ship operates in a specific ice thickness category during the considered period (e.g. one year). It is important to note that the frequency of impacts used in this calculation are determined based on the ice impact interval of the considered dataset (e.g. 10-minute intervals for analysis based on MV S.A. Agulhas II data or 20-min intervals for MV Uikku data).

Table 3 presents a summary of the measured distance and frequency of ship-ice impacts per ship, hull area, and ice thickness category. In accordance with the table, for both ships and all ice thickness categories, the number of impacts at the bow area is somewhat higher than at the stern shoulder area. The frequency of impacts at the bow area is lower for MV Uikku than for MV S.A. Agulhas II, which is attributed here to the fact that the MV Uikku was escorted by an icebreaker whereas MV S.A. Agulhas II operated independently without icebreaker assistance. This is also reflected in the ratio of bow to stern shoulder impacts for the MV Uikku, which are on average 17% lower than the ratio of bow to stern shoulder impacts MV S.A. Agulhas II, which reflects how icebreaker

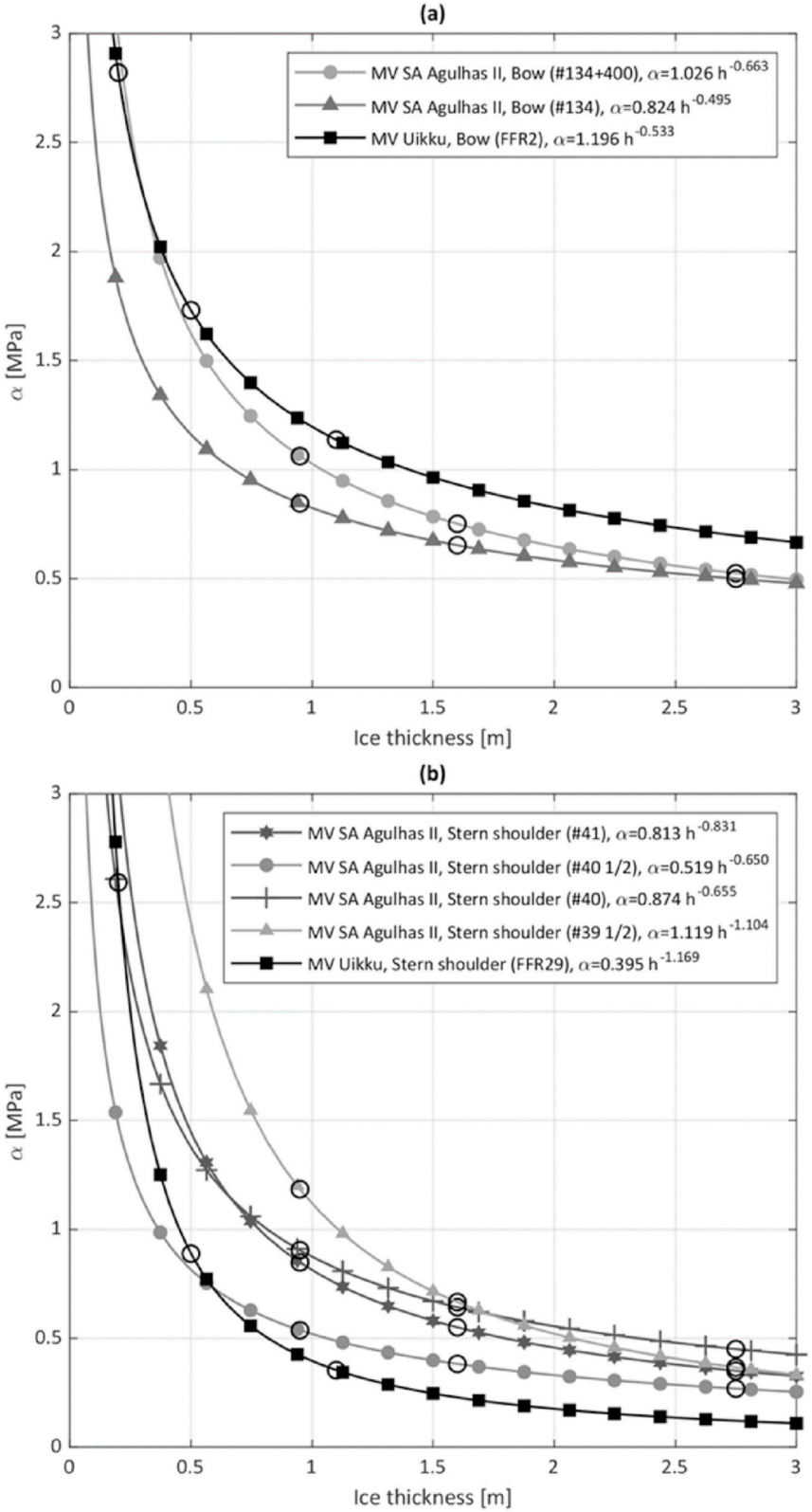

Fig. 13. Dependencies between α and ice thickness (h) for (a) the bow, and (b) the stern shoulder areas of MV S.A. Agulhas II and MV Uikku. The circles indicate the measured points to which the curves are fitted.

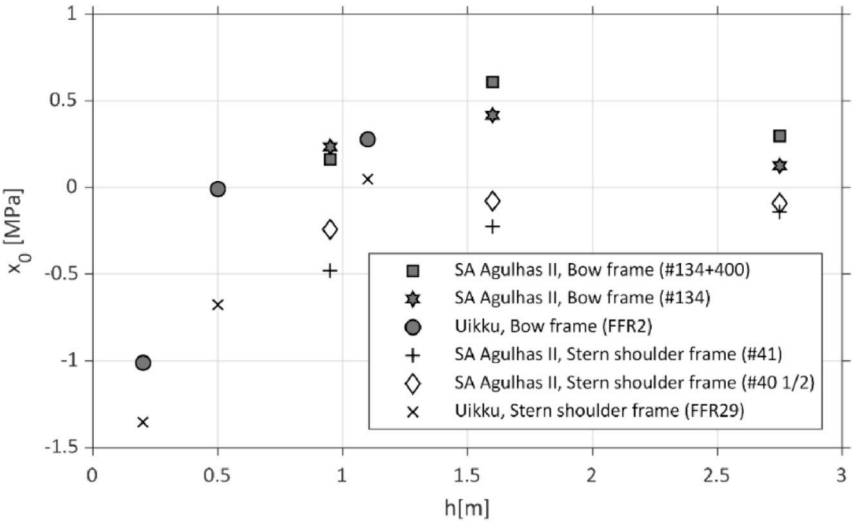

Fig. 14. The relation between x_0 and h for different ships and hull areas.

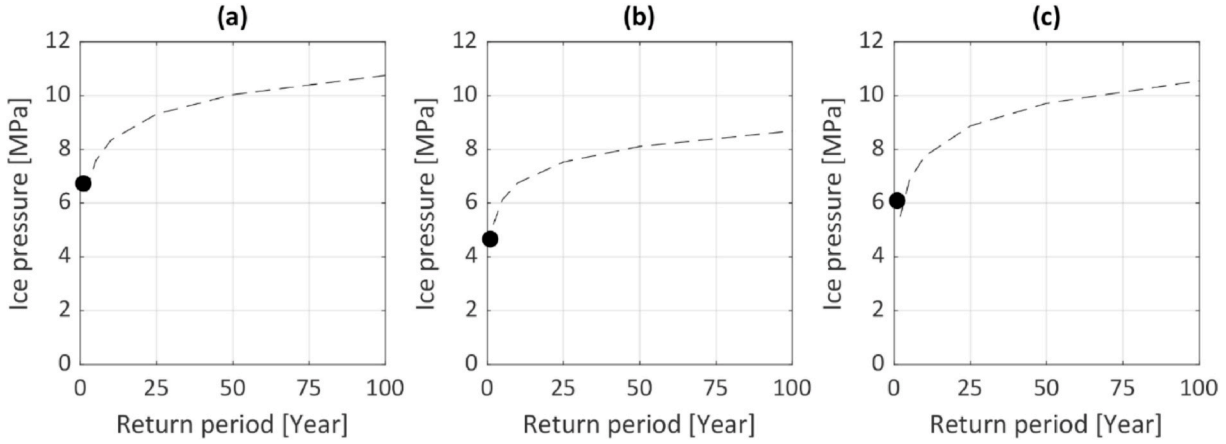

Fig. 15. Comparison of the estimated annual maximum local pressures corresponding to different return periods for the ice thickness of 1.0 m (dashed line) with the maximum of the full-scale 10- and 20-min maximum ice pressures (black dot) for (a) MV S.A. Agulhas II bow frame (#134 + 400), (b) MV S.A. Agulhas II bow frame (#134), and (c) MV Uikku bow frame (FFR2).

escorts can potentially reduce the exposure of a vessel's bow to ice impacts.

2.7. *Estimated annual maximum local pressure vs maximum measured ice pressure*

Based on the preceding analyses, annual local ice pressures corresponding to different return periods have been calculated for the bow regions of both MV S.A. Agulhas II and MV Uikku. For the purpose of this example, ice pressures have been calculated for an ice thickness of 1.0 m for return periods in the range of 1–100 years. For the measurements from MV S.A. Agulhas II and MV Uikku, an ice thickness of 1.0 m corresponds to ice thickness categories 1 and 3, respectively. As per Fig. 15, the estimated extreme local pressure values are plotted along with the maximum measured ice pressure from the corresponding data set. Overall there is good agreement and the measured maximum generally corresponds with estimates corresponding to 1–5 year return periods. A similar comparison for the stern shoulder region is presented in Fig. 16, which also shows good agreement between maximum values from measured data and estimates corresponding to 1–5 year return periods. It is noted that for the sample calculations shown here, the relatively large differences between the estimated pressures for the bow and the stern shoulder may be attributed to differences in α and the number of ice impacts.

Fig. 17 shows how the maximum local ice pressure for various return periods depends on the ice thickness and hull location. Like the area – pressure curves presented in Fig. 12, the curves presented in Fig. 17 are calculated both for (a) the bow area of MV SA Agulhas II (#134 + 400) and MV Uikku (FFR2), and (b) for the stern shoulder area of MV SA Agulhas II (#41) and MV Uikku (FFR29). As per Table 3, the annual number of impacts on the bow of MV SA Agulhas II (#134 + 400) and MV Uikku (FFR2) are determined

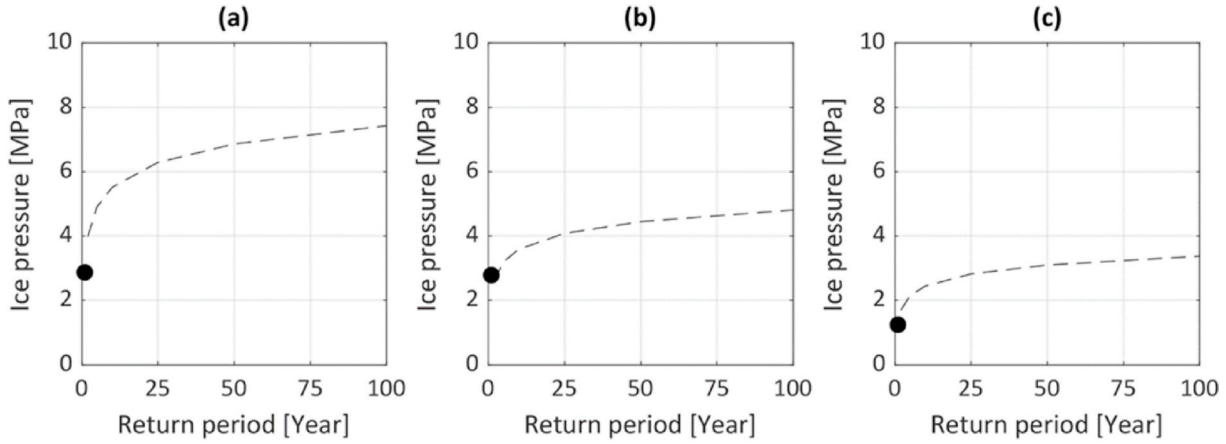

Fig. 16. Comparison of the estimated maximum local pressures for the ice thickness of 1.0 m (dashed line) with the maximum of the full-scale 10- and 20-min maximum ice pressures (black dot) for (a) MV S.A. Agulhas II stern shoulder frame (#41), (b) MV S.A. Agulhas II stern shoulder frame (#40 ½), MV Uikku stern shoulder frame (FFR29).

based on the measurements as 1428 and 109, respectively. The corresponding annual number of impacts on the stern shoulder of MV SA Agulhas II (#41) and MV Uikku (FFR29) are 1063 and 97, respectively.

In Table 4 and Table 5, the 25-year maximum pressure has been estimated for different ice categories for the bow and stern shoulder of MV S.A. Agulhas II and MV Uikku. For both ships, as anticipated, the highest expected pressure is on the bow and corresponds to the exposure associated with the thinner ice category for each vessel. For MV S.A. Agulhas II, the maximum pressure on the stern shoulder is around 24% lower than on the bow, whereas the corresponding value for MV Uikku is 13% lower. The maximum pressures determined for the bow and stern shoulder of MV Uikku are higher or similar than those determined for MV S.A. Agulhas II. This is because the ice thickness categories B1–B2 represent lower ice thicknesses than those of the thickness categories A1-A3. On the other hand, the ice thickness category A1, with a mean ice thickness of 0.95 m, and the ice thickness category B3, with a mean ice thickness of 1.1 m, are comparable. As per Table 4, the 25-year maximum pressures on the bow and stern shoulder of MV S.A. Agulhas II related to exposure to ice of category A1 are 9.3 MPa and 7.1 MPa, respectively. As per Table 5, the corresponding values for MV Uikku related to exposure to ice of category B3 are 7.9 MPa and 2.5 MPa. Thus, for the comparable ice thickness categories A1 and B3, we find that the 25-year maximum pressure on the bow and stern shoulder of MV Uikku are around 15% and 65% lower than corresponding pressures on MV S.A. Agulhas II. The lower pressures on MV Uikku are here attributed to the fact that the MV Uikku was escorted by an icebreaker whereas MV S.A. Agulhas II operated independently.

2.8. Sensitivity analysis

A sensitivity analysis has been conducted to assess how sensitive the estimated maximum local pressure is to variations in the distance covered in ice and the resulting number of ice impacts (μ). Specifically, in accordance with Table 6, the maximum local pressure for a 25-year return period on the bow area of MV S.A. Agulhas II is estimated for two alternative scenarios with respect to the number of ice impacts (μ). In scenario 1, it is assumed that the distances traveled in ice of various thicknesses and hence also the μ –values are one-tenth of those of the measurement voyage. In scenario 2, it is assumed that the distances traveled in ice of various thicknesses and the related μ –values are 10-times larger than those of the measurement voyage. As per Table 6, such variations in the assumed distance traveled in ice results in variations of around $\pm$25% in the predicted 25-year maximum local pressure. This implies that in the practical application of the event maximum-method, results are not particularly sensitive to the specific number of events, but rather the method is expected to yield a reasonable ice load estimate as long as the estimate of ice exposure is to the correct order of magnitude.

3. Discussion and conclusion

In this study, the event-maximum method, which is a semi-empirical probabilistic method for the estimation of ice loads on structures, has been extended and applied for the analysis of contact ship-ice data. To achieve this, a new definition for line-load area was introduced which has been used to determine ice pressure values from these data. Pressure-area results obtained using this line-load area definition were compared to pressure-area results obtained using local design area definition for similar ice conditions and found to yield a good general agreement.

Two different sets of full-scale ice load measurements, namely measurements recorded on a voyage across the Antarctic Ocean, and measurements recorded on a voyage across the Barents Sea and the Kara Sea, have been analyzed. Based on the load measurements and the event-maximum method, a set of α-area curves have been developed to model the relationship between the line-load area and the maximum nominal ice pressure. For both data sets, α-area curves were calculated for two different hull locations, namely the bow and

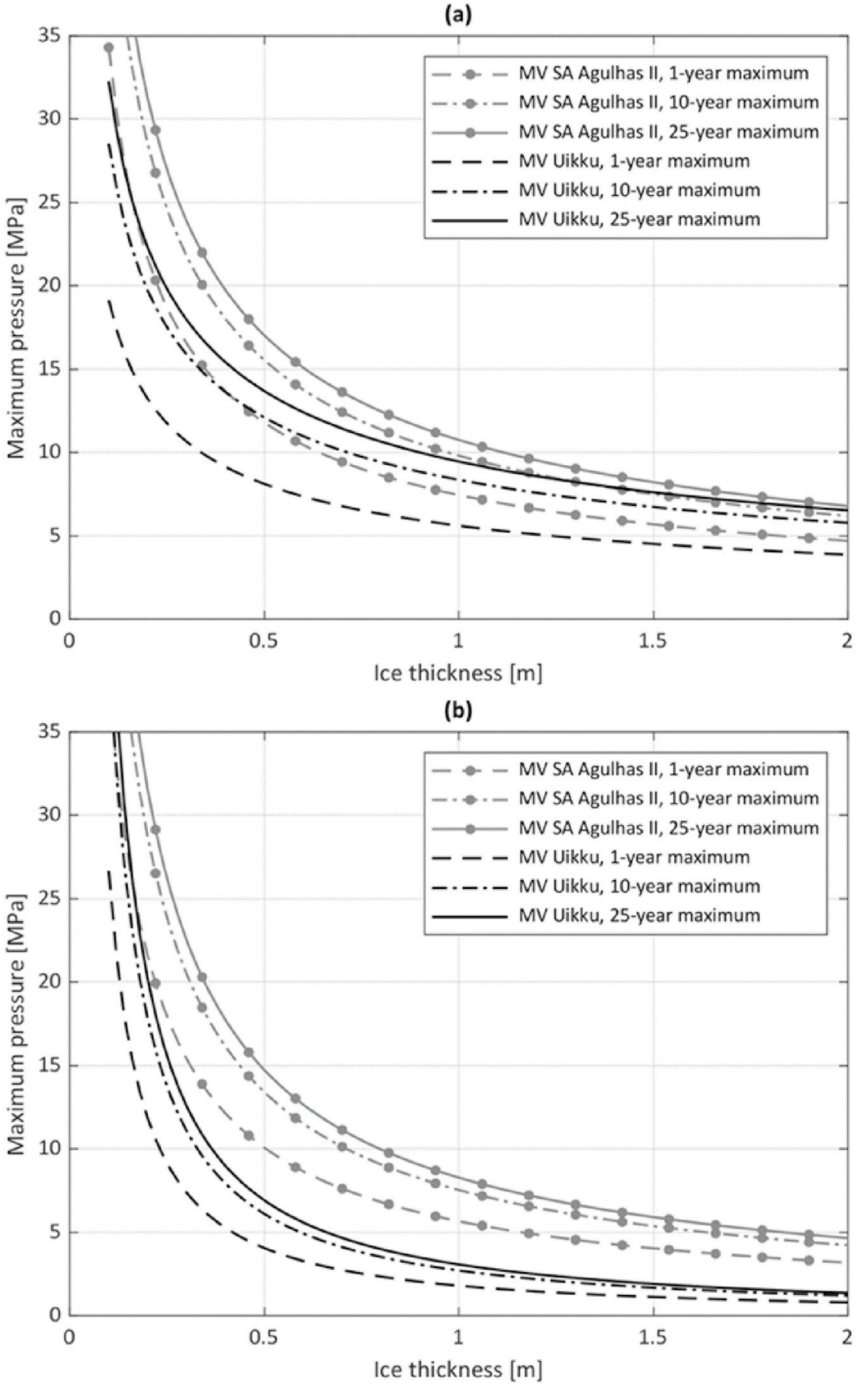

Fig. 17. Maximum local pressure for the return period of 1, 10, and 25 years at (a) bow, and (b) stern shoulder area of MV SA Agulhas II and MV Uikku.

the stern shoulder, and two different types of operations, namely independent operation in ice and icebreaker assisted operation in ice.

The event-maximum method was further extended to assess the relationship between the peak nominal ice pressure and ice thickness. To this end, two main assumptions were made. First, it was assumed that each measured maximum ice load corresponds to the maximum ice thickness observed during the same period. Second, in accordance with the Finnish-Swedish ice class standard 1A super, it was assumed that during a given ship-ice interaction, the ice load height is 30% of the ice thickness. From this analysis, it was observed that calculated α-h curves show a clear negative correlation between ice thickness and local ice pressures, which is consistent

Table 4
Estimated 25-year maximum local ice pressure on the bow and stern shoulder of MV S.A. Agulhas II.

Ice thickness category	A1	A2	A3
Mean ice thickness [m]	0.95	1.60	2.75
Time [years]	25	25	25
$F_Z(z_e)$	$1-\frac{25}{100}=0.960$	$1-\frac{25}{100}=0.960$	$1-\frac{25}{100}=0.960$
$-\ln[-\ln\ F_Z(z_e)]$	3.20	3.20	3.20
x_0 [MPa]	0	0	0
Bow (#134 + 400)			
α [MPa]	1.05	0.75	0.5
μ	285	699	444
$\ln\mu$	5.65	6.55	6.10
z_e **[MPa]**	**9.3**	**7.3**	**4.6**
Stern shoulder (#41)			
α [MPa]	0.85	0.55	0.35
μ	175	529	359
$\ln\mu$	5.16	6.27	5.88
z_e **[MPa]**	**7.1**	**5.2**	**3.2**

Table 5
Estimated 25-year maximum local ice pressure on the bow and stern shoulder of MV Uikku.

Ice thickness category	B1	B2	B3
Mean ice thickness [m]	0.20	0.50	1.10
Time [year]	25	25	25
$F_Z(z_e)$	$1-\frac{25}{100}=0.960$	$1-\frac{25}{100}=0.960$	$1-\frac{25}{100}=0.960$
$-\ln[-\ln\ F_Z(z_e)]$	3.20	3.20	3.20
x_0 [MPa]	0	0	0
Bow (FFR2)			
α [MPa]	2.8	1.7	1.1
μ	24	31	54
$\ln\mu$	3.18	3.43	3.99
z_e **[MPa]**	**17.9**	**11.3**	**7.9**
Stern shoulder (FFR29)			
α [MPa]	2.6	0.9	0.35
μ	16	28	53
$\ln\mu$	2.77	3.33	3.97
z_e **[MPa]**	**15.5**	**5.9**	**2.5**

with pressure-thickness trends observed in offshore structure ice pressure measurements and also as predicted from probabilistic fracture mechanics analyses [25].

Calculated α-h curves were applied using the extended event-maximum method to probabilistically estimate the maximum nominal ice pressure on a ship using ice exposure (impact frequency and distance) values based on full-scale ship-ice data for sea ice of various thickness. The peak ice pressures for the above-mentioned cases were calculated for return periods in the range of 1–100 years. These calculated annual maximum values as a function of return period were compared with corresponding full-scale ice load measurements. From this analysis, it was found that the maximum measured pressures are in the same range as the estimated annual maximum corresponding to a return period of 1–5 years. This suggests that this is a promising approach and further work is needed to validate this approach for longer return periods and different exposure bases.

Using the obtained α-h curves, and the number of impact events estimated from full-scale data, corresponding 25-year peak ice pressures were calculated to explore the effects of location and operation type for selected sample conditions. From this result, it was found that the location of the ship-ice impact area on the hull has a relatively small effect on the shape of the corresponding *α-area* curve. This indicates that, if subjected to a similar number of ice impacts, both hull locations are expected to be subject to a similar level of ice loading. However, in accordance with the considered full-scale ice load measurements from MV S.A. Agulhas II and MV Uikku, the number of impacts on the bow is higher than on the stern. As a result, the estimated peak pressure on MV S.A. Agulhas II's stern shoulder is around 24% lower than on the bow, whereas the estimated peak pressure on MV Uikku's stern shoulder is around 13% lower than on the bow.

To analyze the effect of icebreaker assistance on the estimated maximum ice pressure, the 25-year maximum pressures on the bow

Table 6
The effect of the value of μ on the estimated maximum local pressure at the bow area (frame #134 + 400) of MV S.A. Agulhas II.

	Ice thickness category	A1	A2	A3
	x_0 [MPa]	0	0	0
	α [MPa]	1.05	0.75	0.5
	Time [years]	25	25	25
	$F_Z(z_e)$	$1-\frac{25}{100}=0.960$	$1-\frac{25}{100}=0.960$	$1-\frac{25}{100}=0.960$
	$-\ln[-\ln\ F_Z(z_e)]$	3.20	3.20	3.20
Measurement	μ	285	699	444
Voyage	$\ln\mu$	5.65	6.55	6.10
	z_e **[MPa]**	**9.3**	**7.3**	**4.6**
Scenario 1	μ	28.5	69.9	44.4
	$\ln\mu$	3.35	4.25	3.79
	z_e **[MPa]**	**6.9**	**5.6**	**3.5**
	Deviation [%]	−26%	−24%	−25%
Scenario 2	μ	2850	6990	4440
	$\ln\mu$	7.96	8.85	8.40
	z_e **[MPa]**	**11.7**	**9.0**	**5.8**
	Deviation [%]	26%	24%	25%

and stern shoulder of MV Uikku are compared to those of MV S.A. Agulhas II. The results indicate that for exposure to ice of similar thickness, the estimated 25-year maximum pressure on the bow and stern shoulder of MV Uikku are around 15% and 65% lower than the corresponding pressures on MV S.A. Agulhas II. The lower pressures on MV Uikku are here attributed to the fact that the MV Uikku was escorted by an icebreaker whereas MV S.A. Agulhas II operated independently. Further study of this effect is recommended to better understand how having icebreaker support affects vessel navigation and links to exposure. Since the exposure of the stern shoulder to extreme ice loads is expected to be higher for vessels that have a higher number of turning events per NM along its route, it would be of interest to assess if there is a systematic difference if a vessel is following in the broken ice channel behind an icebreaker versus charting its own independent route. This aspect should be given further consideration in future work.

During the voyage considered in this study, the independently operating ship MV S.A. Agulhas II received no icebreaker assistance. Whenever she encountered heavy ice, she was either able to pass through the ice field on her own, or she chose another path. Anyhow, any ship operating in ice might occasionally get stuck due to high ice resistance. In terms of ice loading, this is important to consider as a ship beset in ice might be subject to significant compressive ice loads. The assessment of such compressive loads is a topic for future research.

Due to the empirical nature of the present approach, its ability to consider specific ice loading factors is limited by the availability of related data. For instance, in order to assess the effect of a specific ice loading control measure (e.g. crew measures to reduce ice loading), for the same operating conditions, the approach would require two different series of full-scale ice load measurements: one in which the measure is implemented, and one in which it is not. In order to limit the required amount of data, a better understanding of what factors are important enough to motivate specific consideration should be established in future studies.

In summary, it is hoped that the presented analysis and approach contribute towards the goal-based structural design of Arctic ships by extending the application of the principles of the event-maximum method and applying this approach to the analysis of full-scale ship-ice load measurements. In modifying this approach to assess ice pressure based on ice thickness, it becomes possible to estimate a ship's level of ice loading based on its actual ice exposure determined in terms of the distance traveled in sea ice of various types and thicknesses. However, future research and development is necessary to increase the applicability, accuracy, and reliability of the proposed approach. As with any empirical method, the results of these analyses are explicitly linked to the conditions associated with the data from which the relationships are derived. For further validation, additional analysis of new and existing long-term full-scale ice load measurements are needed, including providing a more detailed treatment of exposure to better allow for the application of empirical curves to conditions other than those associated with one specific dataset. Additional full-scale ice load measurements are also needed to determine additional α-h curves for different types of ships (e.g. bulbous bow vs. icebreaking bow), different geographical areas (e.g. the Baltic Sea), different ice types (e.g. brash ice, first-year ice, first-year ice with multi-year ice intrusions, multi-year ice), and operating modes (icebreaker assistance vs. independent operation). As demonstrated by Shamaei et al. [23]; the assumed ice load height also has a moderate effect on calculated peak ice pressure, and further studies on the relationship between ice thickness and load height are recommended to reduce the related uncertainty.

Declaration of competing interest

The authors have no conflicts of interest to declare.

Acknowledgments

This project has received funding from the Lloyd's Register Foundation, a charitable foundation, helping to protect life and property by supporting engineering-related education, public engagement and the application of research www.lrfoundation.org.uk. The project has also received funding from the European Union's Horizon 2020 research and innovation programme under Grant Agreement number: 723526 (Project name: SEDNA - Safe maritime operations under extreme conditions: the Arctic case).

References

[1] ARCDEV. *Final public report of the ARCDEV project,* Espoo: ARCDEV consortium. 1998.
[2] IMO. International code for ships operating in polar waters (Polar Code). MEPC 68/21/Add.1 Annex 10. London: International Maritime Organization; 2015.
[3] Kujala P, et al. Review of risk-based design for ice-class ships. Mar Struct 2019;63:181–95.
[4] Kujala P. On the statistics of ice loads on ship hull in the Baltic. Helsinki: Helsinki University of Technology; 1994.
[5] Taylor R, Jordaan I, Li L, Sudom D. Local design pressure for structures in ice. Offshore Mechanics and Arctic Engineering 2010;132.
[6] Jordaan I, Maes M, Brown P, Herman I. Probabilistic analysis of local ice pressure. Offshore Mechanics and Arctic Engineering 1993;115.
[7] Sanderson TJO. Full-scale measurements. Teoksessa: *Ice mechanics- Risk of offshore structures*. London: Graham and Tortman; 1988. p. 140.
[8] Frederking R, Jordaan I, Js M. *Field test of ice indentation at medium scale Hobson's Choics Ice Island.* Espoo. Proc. IAHR international symphosium on ice. 1990.
[9] Daley C, St John J, Blount H. Ice loads and ship response to ice. Washington, DC: Ship Structures Committee; 1990.
[10] Jordaan I, et al. Principles for local and global ice design using pressure area relationships. Potsdam: POAC; 2005.
[11] Taylor RS, Richard M, Hossain R. A probabilistic high-pressure zone model for local and global loads during ice-structure interactions. J Offshore Mech Arctic Eng 2019;141(5).
[12] Ralph F. Design of ships and offshore structures: a probabilistic approach for multi-year ice and iceberg impact loads for decision-making with uncertainty. St. John's: Memorial University; 2016.
[13] Kujala P, Vuorio J. Results and statistical analysis of ice load measurements on board icebreaker Sisu in winters 1979 to 1985. Helsinki: Technical Research Centre of Finland; 1986.
[14] Suominen M, Kujala P. *Analysis of short-term ice load measurements on board MS Kemira during the winters 1987 and 1988,* Espoo. Aalto University, School of Science and Technology, Department of Applied Mechanics; 2010.
[15] Suyuthi A, Leira B, Riska K. Statistics of local ice load peaks on ship hulls. Struct Saf 2012;40:1–10.
[16] Kotilainen M, Vanhatalo J, Suominen M, Kujala P. Predicting ice-induced load amplitudes on ship bow conditional on ice thickness and ship speed in the Baltic. Cold Reg Sci Technol 2017;135:116–26.
[17] Traficom. Ice class regulations and the application thereof. Helsinki: Traficom - Finnish Transprot Safety Agency; 2017.
[18] ISO. Petroleum and natural gas industries — Arctic offshore structures. Geneva: International Organization for Standardization; 2010.
[19] Bergström M, Erikstad S, Ehlers S. A simulation-based probabilistic design method for Arctic Sea transport systems. Marine Science and Application 2016;15(4):349–69.
[20] Kujala P, Kulovesi J, Lehtiranta J, Suominen M. *Full-scale measurements on board S.A. Agulhas II in the Antarctic waters 2013-2014,* Espoo. Aalto University; 2014.
[21] Hänninen S, Lensu M, Riska K. Analysis of the ice load measurements during USCGC Healy ice trials, spring 2000. Espoo: Helsiki University of Technology, Ship Labratory; 2001.
[22] Kotisalo K, Kujala P. Ice load measurement onboard MT Uikku, Mesearment results from the ARCDEV voyage to Ob-estuary. Ship labratory: Helsinki University of Technology; 1999.
[23] Shamaei F, et al. Analysis of the event-maximum method for the prediction of local pressures on a ship's hull in the Antarctic ice. In: Proceedings of the 25th International Conference on Port and Ocean Engineering under Arctic Conditions (POAC 2019), Delft; 2019.
[24] IACS. Requirements concerning POLAR CLASS. London: International Association of Classification Societies; 2016.
[25] Taylor RS, Jordaan IJ. Probabilistic fracture mechanics analysis of spalling during edge indentation in ice. Eng Fract Mech 2015;134:242–66.